cTAGE5 deletion in pancreatic β cells impairs proinsulin trafficking and insulin biogenesis in mice

Junwan Fan,[1,3]* Yaqing Wang,[1]* Liang Liu,[1,3] Hongsheng Zhang,[1,3] Feng Zhang,[1,3] Lei Shi,[1] Mei Yu,[1,3] Fei Gao,[2] and Zhiheng Xu[1,4]

[1]State Key Laboratory of Molecular Developmental Biology, CAS Center for Excellence in Brain Science and Intelligence Technology, Institute of Genetics and Developmental Biology and [2]State Key Laboratory of Reproductive Biology, Institute of Zoology, Chinese Academy of Sciences, Beijing, China
[3]University of Chinese Academy of Sciences, Beijing, China
[4]Parkinson's Disease Center, Beijing Institute for Brain Disorders, Beijing, China

Proinsulin is synthesized in the endoplasmic reticulum (ER) in pancreatic β cells and transported to the Golgi apparatus for proper processing and secretion into plasma. Defects in insulin biogenesis may cause diabetes. However, the underlying mechanisms for proinsulin transport are still not fully understood. We show that β cell–specific deletion of *cTAGE5*, also known as *Mea6*, leads to increased ER stress, reduced insulin biogenesis in the pancreas, and severe glucose intolerance in mice. We reveal that cTAGE5/MEA6 interacts with vesicle membrane soluble *N*-ethyl-maleimide sensitive factor attachment protein receptor Sec22b. Sec22b and its interaction with cTAGE5/MEA6 are essential for proinsulin processing. cTAGE5/MEA6 may coordinate with Sec22b to control the release of COPII vesicles from the ER, and thereby the ER-to-Golgi trafficking of proinsulin. Importantly, transgenic expression of human cTAGE5/MEA6 in β cells can rescue not only the defect in islet structure, but also dysfunctional insulin biogenesis and glucose intolerance on *cTAGE5/Mea6* conditional knockout background. Together our data provide more insight into the underlying mechanism of the proinsulin trafficking pathway.

Introduction

Diabetes mellitus is a set of metabolic disorders, including type 1 diabetes and type 2 diabetes (Ashcroft and Rorsman, 2012). Type 1 diabetes is usually caused by the destruction of insulin-producing cells in the pancreas. Type 2 diabetes is connected with both pancreatic β cell dysfunction and peripheral insulin resistance (Kusminski et al., 2009; Lindahl et al., 2014; Morley et al., 2015). Insulin is a peptide hormone, produced by pancreatic β cells, which is indispensable for proper maintenance of glucose homeostasis (Heit et al., 2006; Li et al., 2014; Ye et al., 2014). Proinsulin, the precursor of insulin, is rapidly translocated into ER, where it undergoes oxidative folding by forming three disulfide bonds (Gupta et al., 2010; Liu et al., 2014). Only properly folded proinsulin can be assembled into COPII vesicles and transported from ER to Golgi (Fang et al., 2015). Increases in misfolded proinsulin in the ER would perturb the ER environment and lead to ER stress (Scheuner et al., 2005; Sun et al., 2015). The mechanism of insulin biosynthesis and glucose-stimulated insulin secretion has been well studied, yet much less is known about the proinsulin trafficking in the secretory pathway.

ER-to-Golgi transport of COPII vesicles requires the docking and fusing machinery to form the vesicular tubular clusters and the fusion of vesicular tubular clusters with cis-Golgi (Xu and Hay, 2004; Wang et al., 2015). SNARE complexes play a pivotal role in membrane fusion throughout the secretory pathway (Xu et al., 2000; Joglekar and Hay, 2005; Jahn and Scheller, 2006; Wickner and Schekman, 2008). In mammalian cells, the v-SNARE Sec22b, t-SNARE Syntaxin5, Membrin, and Bet1 form a characterized quaternary complex that participates in the anterograde ER-to-Golgi transport (Bentley et al., 2006; Adolf et al., 2016). However, whether the ER/Golgi SNARE is involved in proinsulin trafficking, and how this process is regulated, are still not clear.

cTAGE5 was identified originally as *Meningioma-expressed antigen 6* (*Mea6*) and it has been reported to be up-regulated in several cancer tissues or cell lines. *cTAGE5/Mea6* is postulated as a potential oncogene (Comtesse et al., 2002; Usener et al., 2003; Saliminejad et al., 2013). Recent studies have shown that cTAGE5 is localized at ER exit sites (ERESs) and participates in collagen secretion (Saito et

*J. Fan and Y. Wang contributed equally to this paper.

Correspondence to Zhiheng Xu: zhxu@genetics.ac.cn; Yaqing Wang: yqwang@genetics.ac.cn

Abbreviations used: BFA, Brefeldin A; cKO, conditional knockout; coIP, co-immunoprecipitation; ERES, ER exit site; H&E, hematoxylin and eosin; IPGTT, intraperitoneal glucose tolerance test; IPITT, intraperitoneal insulin tolerance test; PDI, protein disulfide isomerase; TEM, transmission electron microscopy; VLDL, very-low-density lipoprotein.

The Rockefeller University Press
J. Cell Biol. Vol. 216 No. 12 4153–4164
https://doi.org/10.1083/jcb.201705027

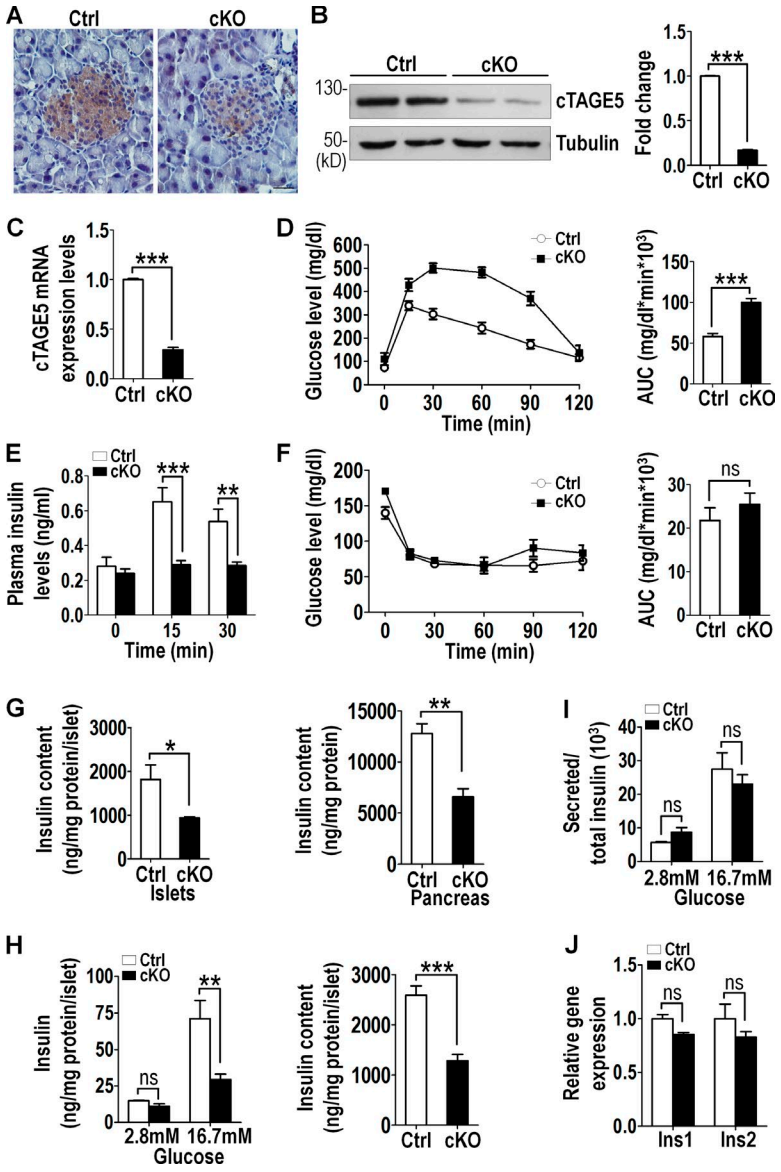

Figure 1. ***cTAGE5* cKO leads to reduced insulin biogenesis and glucose intolerance.** All mice used here were 8-wk-old male mice. (A) cTAGE5 expression was analyzed by immunohistochemistry on pancreas sections. Ctrl, control. Bar, 20 µm. (B) Western blotting analysis of cTAGE5 expression in isolated islets. Quantitation of cTAGE5 protein levels normalized to tubulin loading control shown at right. (C) Relative *cTAGE5* mRNA expression in isolated islets detected by real-time PCR (n = 4). (D) IPGTT was performed. Area under the curve (AUC) shown at right (Ctrl and cKO, n = 10). (E) Plasma insulin levels in control (n = 6) and cKO (n = 10) mice during IPGTT. (F) IPITT was performed. Area under the curve shown at right (Ctrl and cKO, n = 6). (G) Total insulin content in isolated islets and pancreas (Ctrl and cKO, n = 4). (H) Isolated islets were cultured in vitro (Ctrl and cKO, n = 9). Glucose-stimulated insulin secretion and total insulin content were measured. (I) Glucose-stimulated insulin secretion was normalized by total insulin content. (J) Relative *Ins1* and *Ins2* mRNA expression in isolated islets was analyzed by real-time PCR (Ctrl and cKO, n = 4). All data are means ± SEM (Student's t test) from three independent experiments. *, $P < 0.05$; **, $P < 0.01$; ***, $P < 0.001$; ns, not significant.

al., 2011, 2014). In addition, cTAGE5/MEA6 plays a critical role in COPII assembly and the transportation of very-low-density lipoprotein (VLDL) from ER to Golgi (Santos et al., 2016; Wang et al., 2016).

Here we show that conditional knockout (cKO) of *cTAGE5/Mea6* in pancreatic β cells leads to glucose intolerance as a result of the disruption of proinsulin trafficking and reductions in glucose-stimulated insulin secretion. We provide evidence that cTAGE5/MEA6 interacts and is likely to coordinate with Sec22b to play an essential role in proinsulin trafficking from ER to Golgi.

Results

cTAGE5 ablation in pancreatic β cells leads to reduced insulin biogenesis and glucose intolerance

cTAGE5 is mainly expressed in the pancreas and liver, and previous work has shown that deletion of *cTAGE5* in hepatocytes leads to fatty liver disease (Wang et al., 2016). We therefore investigated the biological function of cTAGE5 in the pancreas. *cTAGE5* was specifically deleted in pancreatic β cells by crossing *cTAGE5*$^{\Delta/+}$*; Insulin2 (Ins2)-Cre* with *cTAGE5*$^{Flox/Flox}$ mice (Wang et al., 2016), which generated four different offspring lines (*cTAGE5*$^{FL/\Delta}$*; Ins2-Cre*, *cTAGE5*$^{FL/+}$*; Ins2-Cre*, *cTAGE5*$^{FL/+}$, and *cTAGE5*$^{FL/\Delta}$). Decreased cTAGE5 expression was confirmed by immunohistochemistry in *cTAGE5*$^{FL/\Delta}$*; Ins2-Cre* mice compared with *cTAGE5*$^{FL/+}$ mice, which are referred to hereafter as cKO and control, respectively (Fig. 1 A). Western blotting and real-time PCR analysis also confirmed the substantially reduced levels (∼70–80%) of cTAGE5 expression in isolated islets (Fig. 1, B and C). Gross evaluation showed *cTAGE5* cKO mice were phenotypically unremarkable, although their body weights were lower than those of their control littermates up to 1 yr old (Fig. S1 A).

Because pancreatic β cells in the islets of Langerhans are the primary source of insulin, which maintains metabolic homeostasis, we explored the effect of *cTAGE5* deletion in β cells on glycemic control. cKO mice on a regular chow diet exhibited higher glucose levels than control mice. During intraperitoneal glucose tolerance tests (IPGTTs), both male and female cKO

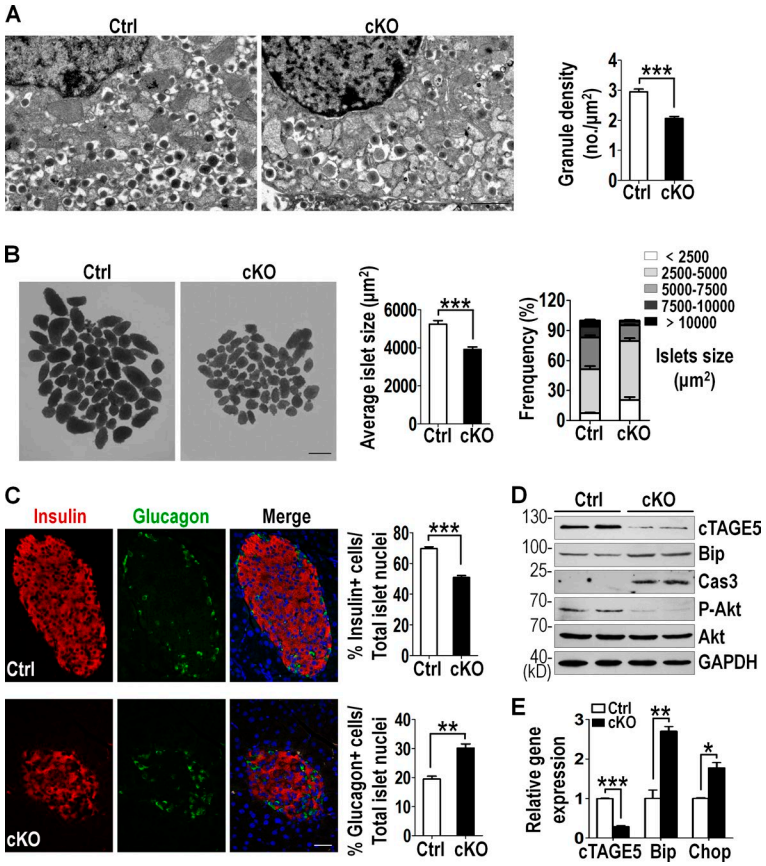

Figure 2. **Abnormal islet morphology and ER stress in *cTAGE5* knockout mice.** (A) TEM of isolated islets (control [Ctrl] and cKO, $n = 5$). Bar, 1 µm. Quantitation of the density of insulin granules per β cell is shown at right (Ctrl, $n = 60$; cKO, $n = 85$). (B) The mean islet size and the percentage of islet size distribution (Ctrl and cKO, $n = 7$). Bar, 200 µm. (C) Pancreas sections stained with insulin (red) and glucagon (green; Ctrl and cKO, $n = 5$). Bar, 100 µm. Quantitation of the percentage of insulin-positive cells ($n = 40$) and glucagon-positive cells ($n = 30$) in islets is shown at right. (D) Western blotting analysis of cTAGE5, Bip, P-Akt, and the activated form of Caspase3 expression in isolated islets. GAPDH served as loading control. (E) Relative *cTAGE5*, *Bip*, and *Chop* mRNA expression in isolated islets analyzed by real-time PCR (Ctrl and cKO, $n = 4$). All data are means ± SEM (Student's *t* test) from more than two independent experiments. *, $P < 0.05$; **, $P < 0.01$; ***, $P < 0.001$.

mice showed significantly higher glucose levels than control mice (Fig. 1 D and Fig. S1 B), whereas their plasma insulin levels were substantially lower (45–55%; Fig. 1 E and Fig. S1 C), suggesting that cKO mice were potentially unable to elevate insulin production in response to the glucose challenge. The possibility of insulin resistance, which can result in glucose intolerance, was excluded by intraperitoneal insulin tolerance test (IPITT) as the cKO mice response normally to insulin (Fig. 1 F and Fig. S1 D). These results indicate that glycemic control is disturbed in cKO mice as a result of the defect in insulin production or secretion, but not in insulin sensitivity.

10-mo-old cKO male mice also showed significantly higher glucose levels in the IPGTT test (Fig. S1 E). Therefore, we performed all the in vivo experiments in this study in 8-wk-old male mice hereafter. Neither the Ins2-Cre mice nor the heterozygous *cTAGE5*$^{FL/\Delta}$ mice had defects in glucose tolerance (Fig. S2 A). Of note, Ins2-Cre has been shown to be expressed in the hypothalamus, which regulates different endocrine functions (Tang et al., 2013; Hasegawa et al., 2014). We generated conditional *cTAGE5* deletion in the brain, including the hypothalamus, by Nestin-Cre and observed that glucose tolerance remained unaffected (Fig. S2, B and C).

We went on to inspect insulin production and found out that the insulin content in islets and pancreas in cKO mice was around 50% lower (Fig. 1 G), but the proinsulin content in islets was similar (Fig. S3 A). To further characterize whether the lower insulin levels in cKO mice were a β cell–autonomous effect, we isolated islets and performed glucose-stimulated insulin secretion in static incubation. The insulin secretion from cKO islets was significantly reduced in the presence of 16.7 mM glucose (Fig. 1 H), consistent with the in vivo observations. Interestingly, after standardizing with total insulin content, the percentage of secreted insulin from cKO islets was similar to controls (Fig. 1 I). This indicates that, during glucose-stimulated insulin secretion, the lower level of insulin in cKO islets is the major cause of reduced insulin secretion.

The defect in insulin biogenesis in cKO islets could be caused by reduced transcription and translation of insulin coding genes. Nevertheless, there were no significant difference in the *Ins1* and *Ins2* mRNA and proinsulin protein levels in isolated cKO and control islets (Fig. 1 J and Fig. S3, B and C). In addition, the mRNA levels of *Vamp2*, *Stx1a*, and *SNAP25*, which are involved in exocytosis, remained unchanged (Fig. S3 D). These results suggest that the production of proinsulin and the exocytotic pathway for insulin are likely unaffected in cKO mice.

Deletion of *cTAGE5* causes ER stress and impairs islet structure

To explore the cause of the significantly reduced insulin content in cKO islets, we inspected the morphology and structure of the islets. Transmission electron microscopy (TEM) showed significantly decreased (around 30%) insulin granule density in cKO β cells (Fig. 2 A). Hematoxylin and eosin (H&E) staining on serial pancreas sections revealed that the control and cKO pancreas comprised a similar number of islets per unit area (Fig. S3 E). However, when the mean sizes of isolated islets were analyzed, the cKO islets were significantly smaller (Fig. 2 B). These data suggest that disturbance of glycemic control in cKO mice is most likely caused by defects in insulin biogenesis as well as the reduced islet mass in the pancreas.

Intriguingly, during the islet isolation procedure, we found that the cKO islets were less compact and tended to get

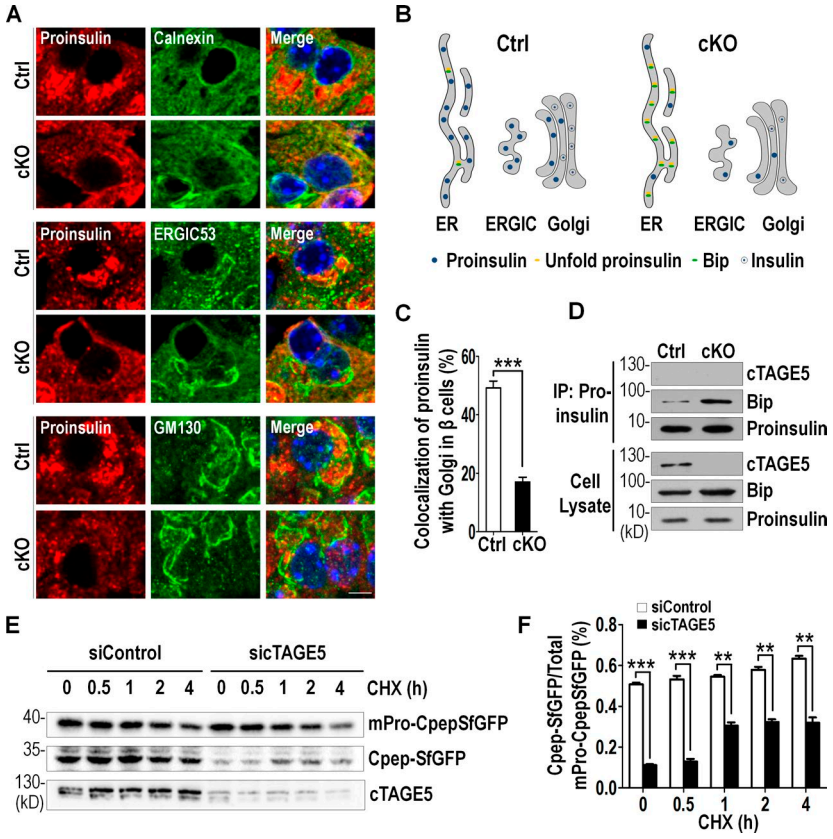

Figure 3. **The defect of proinsulin trafficking in *cTAGE5* knockout mice.** (A) Pancreas sections immunostained with Proinsulin (red) and Calnexin (green), ERGIC53 (green), and GM130 (green; control [Ctrl] and cKO, $n = 6$). Bar, 10 µm. (B) The model of distribution of proinsulin throughout ER-to-Golgi transport pathway. (C) Percentage of the colocalization of Proinsulin with Golgi in β cells from A. (D) The increased interaction between endogenous Proinsulin and Bip in isolated islets was observed by coIP with Proinsulin antibody in cKO islets. (E) MIN6 cells stably expressing scramble shRNA (siControl) or *cTAGE5* shRNA (sicTAGE5) was described in the methods. Both control and cTAGE5 knockdown cells were infected with mPro-CpepSfGFP expressing lentivirus; 48 h later, MIN6 cells were incubated with cycloheximide. The cells were lysed and probed with GFP antibody at the indicated times. Note C-peptide (CpepSfGFP), which reflected the proper folding and cleavage of proinsulin (mPro-CpepSfGFP), was reduced in cTAGE5 knockdown cells. (F) Percentage of CpepSfGFP to total mPro-CpepSfGFP from (E) was quantitated. All data are means ± SEM (Student's *t* test) from three independent experiments. **, $P < 0.01$; ***, $P < 0.001$.

disintegrated relative to the control islets. To reveal whether deletion of *cTAGE5* in pancreatic β cells affected the islet architecture, pancreas sections were immunostained with glucagon and insulin antibodies. The cKO islets displayed an abnormal constitution of α and β cells, with much fewer insulin-expressing cells and disproportionally more glucagon-expressing cells (Fig. 2 C). In addition, many α cells, which are normally confined around the mantles of islets, spread into the middle of cKO islets.

The reduced number of β cells in cKO islets could potentially be caused by reduced proliferation or increased cell death. Immunostaining of the pancreas sections with Ki67, a marker for proliferating cells, revealed no significant difference between the control and cKO islets (Fig. S3 F). In contrast, the activated form of Caspase3 could be detected, which was accompanied by the significantly decreased levels of phosphorylated Akt, a well-known prosurvival kinase, in cKO islets (Fig. 2 D), suggesting that the loss of β cells may be a result of an increase of apoptosis.

We have shown previously that deletion of *cTAGE5* in hepatocytes resulted in the distended and dispersed ER in cells (Wang et al., 2016). This implicated the presence of ER stress and it was confirmed by significantly elevated levels of Bip and protein disulfide isomerase (PDI), the key markers for ER stress (Fig. S4, A–C). Accordingly, we noticed, in cKO islets, significantly elevated protein levels of Bip (Fig. 2 D) and the mRNA levels of *Bip* and *Chop* (Fig. 2 E). These results implicate an association between ER stress and the increase of apoptosis as well as the decrease of islet mass in cKO islets.

cTAGE5 is essential for proinsulin trafficking from ER to Golgi

Proinsulin is synthesized and folded in the ER and then transported from ER to Golgi to form insulin granules (Liu et al., 2014). Recent evidence has suggested that proinsulin trafficking from ER to Golgi was mainly through COPII (Fang et al., 2015). To investigate whether cTAGE5 was involved in proinsulin trafficking, we inspected the distribution of proinsulin in islets through immunostaining with different markers, Calnexin (ER marker), ERGIC53 (ER-Golgi intermediate compartment marker), and GM130 (Golgi marker). Proinsulin was partially colocalized with Calnexin, ERGIC53, and GM130, indicating that it was distributed throughout the transport pathway. However, proinsulin was mainly colocalized with Calnexin, and lost most of the colocalization pattern with ERGIC53 and GM130 (drop by >60%) in cKO β cells (Fig. 3, A–C). This suggests proinsulin trafficking from ER to Golgi is impaired in cKO β cells.

Disturbed anterograde transport of proinsulin would lead to excessive proinsulin aggregating in ER lumen, which would bind to Bip (Gething and Sambrook, 1992; Scheuner et al., 2005). We performed coimmunoprecipitation (coIP) and found that the amount of proinsulin interacting with Bip was enhanced substantially in cKO islets (Fig. 3 D), in support of the notion of a defect in proinsulin trafficking.

Proinsulin is processed in the Golgi by cleavage (Wijesekara et al., 2010; Liu et al., 2014). To further validate the role of cTAGE5 in proinsulin trafficking, we constructed a mouse proinsulin cDNA (mPro) with superfolder GFP fused within the C-peptide (CpepSfGFP). This proinsulin chimera could be processed to insulin and CpepSfGFP, and was used as a reliable proinsulin processing reporter (Liu et al., 2007; Haataja et al., 2013). We knocked down cTAGE5 expression by lentivirus-mediated shRNA targeting *cTAGE5* in MIN6 cells followed by lentivirus-mediated mPro-CpepSfGFP expression. As shown in Fig. 3 (E and F), the levels of CpepSfGFP in cTAGE5 knockdown cells were significantly lower than that in control cells in

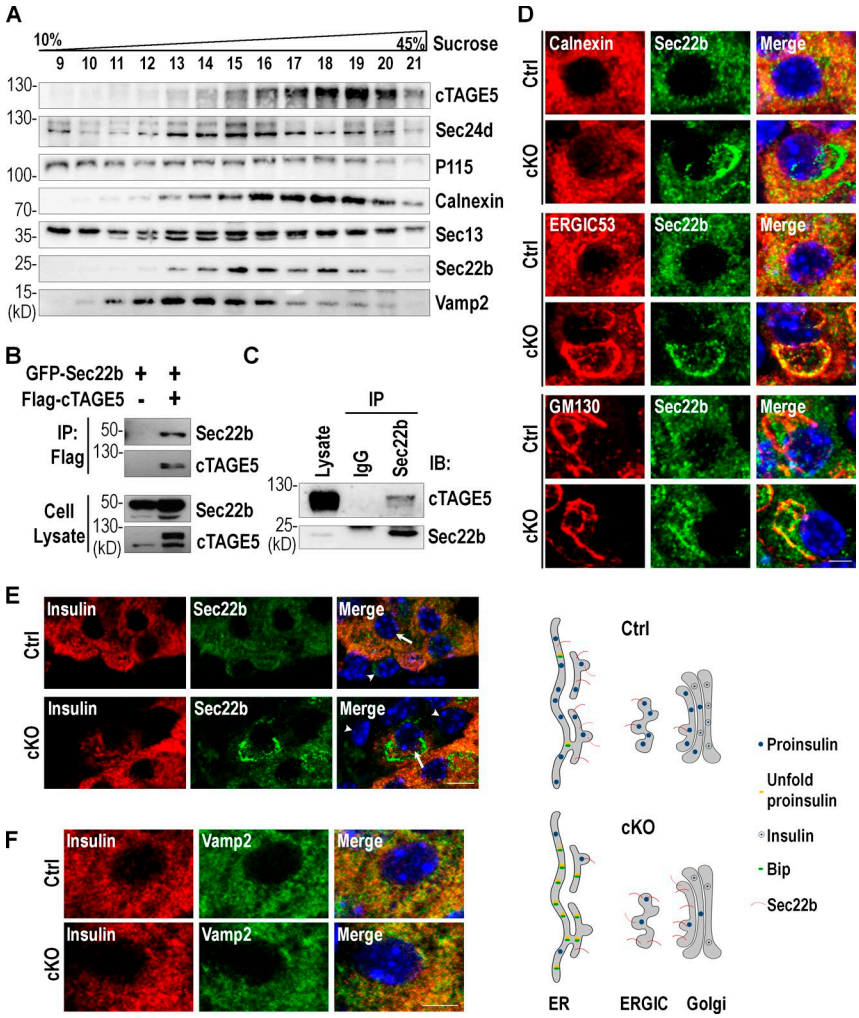

Figure 4. **cTAGE5 interacts with v-SNARE Sec22b and controls its localization.** (A) Subcellular fractionation of MIN6 cells using a continuous sucrose gradient. Data were from three independent experiments with similar results. (B) The interaction of Sec22b with cTAGE5 was assessed by coIP. Constructs expressing Sec22b and cTAGE5 were transfected alone or in combination into 293 cells; 24 h later, cell lysates were precipitated with Flag agarose beads and the immune complexes were detected with Flag or GFP antibody. (C) The interaction between endogenous Sec22b and cTAGE5 in pancreatic islets was observed by coIP with Sec22b antibody. (D) Pancreas sections immunostained with Sec22b (green), Calnexin (red), ERGIC53 (red), and GM130 (red). Data were from three independent experiments with similar results. Bar, 10 µm. The model of distribution of Sec22b throughout ER-to-Golgi transport pathway shown under the figure. (E) Pancreas sections stained with insulin (red) and Sec22b (green). The arrow shows β cell in islets; the arrowhead shows non–β cells in islets. Bar, 20 µm. (F) Pancreas sections stained with insulin (red) and Vamp2 (green). Bar, 10 µm.

the presence of cycloheximide, an inhibitor of protein synthesis. Therefore, our results indicate that cTAGE5 is essential for the anterograde transport of proinsulin from ER to Golgi.

cTAGE5 interacts with Sec22b and controls its cellular localization in β cells

cTAGE5 has been shown to locate on the ERES and interact with COPII components to regulate the transport of VLDL and collagen VII (Santos et al., 2016; Wang et al., 2016). We explored other proteins that might be associated with cTAGE5. A continuous sucrose gradient sedimentation was performed to separate the subcellular fractionations from MIN6 cells. As expected, cTAGE5 was mainly distributed in the ER fraction, overlapping with Calnexin, as well as Sec24d, a cTAGE5-interacting protein (Fig. 4 A). We also noticed that the distribution of Sec22b was similar to that of cTAGE5 and Calnexin, but not Vamp2, a v-SNARE protein participating in Golgi-to-plasma membrane trafficking.

Sec22b is a v-SNARE protein involved in ER-to-Golgi membrane trafficking (Gonzalez et al., 2001; Joglekar and Hay, 2005). Both Sec22b and cTAGE5 have been shown to be capable of forming a complex with COPII components (Mancias and Goldberg, 2007; Wang et al., 2016). We therefore speculated that cTAGE5 might play a role in proinsulin trafficking through interaction with Sec22b. To test this hypothesis, constructs encoding Sec22b and cTAGE5 were transfected into 293 cells individually or in combination, and coIP experiments revealed that Sec22b interacted with cTAGE5 (Fig. 4 B). An interaction between endogenous cTAGE5 and Sec22b was also confirmed (Fig. 4 C).

To investigate whether *cTAGE5* deletion had any effect on Sec22b, we inspected the effect of *cTAGE5* knockout on the localization of Sec22b in pancreatic β cells. As shown in Fig. 4 D, Sec22b had an evenly distributed pattern in β cells, mainly colocalized with Calnexin and ERGIC53, and to a much lesser degree, with GM130. However, its distribution was changed in *cTAGE5* cKO β cells. Sec22b shifted to where ERGIC53 and GM130 were located, while losing most of its colocalization with Calnexin. It seemed that cTAGE5 had a selective role on the localization of Sec22b but not Vamp2 in β cells (Fig. 4, E and F). Although cTAGE5 was important for the distribution of Sec22b, cTAGE5 and Sec22b had no apparent effect on each other's expression levels (Fig. S4, D and E). These results indicate that cTAGE5 is essential for the circulation of Sec22b between the ER and Golgi, and deletion of *cTAGE5* leads to the loss of Sec22b distribution in the ER (Fig. 4 D, bottom).

Sec22b is essential for proinsulin trafficking

Because cTAGE5 interacted with Sec22b and *cTAGE5* deficiency affected Sec22b distribution, we went on to inspect whether the function of Sec22b was essential for proinsulin transport. We knocked down Sec22b expression by lentivirus-mediated

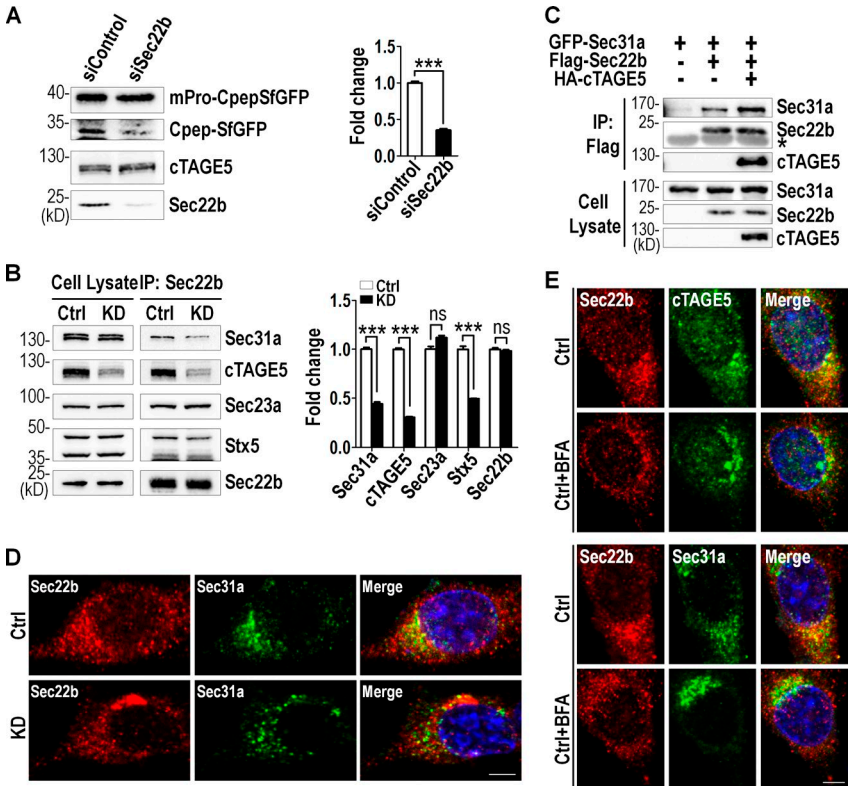

Figure 5. **cTAGE5 depletion affects the Sec22b-SNARE and Sec22b-COPII interaction.** (A) MIN6 cell line stably expressing scramble shRNA (siControl) or *Sec22b* shRNA (siSec22b) was infected with mPro-CpepSfGFP expressing lentivirus. 48 h later, cells were lysed and probed for indicated proteins. Percentage of CpepSfGFP to total mPro-CpepSfGFP is quantitated in the right panel. (B) The interaction of endogenous Sec22b with Sec31a, cTAGE5, Sec23a, and Syntaxin5 in MIN6 cells was observed by coIP with Sec22b antibody. However, the interaction with Sec31a and Syntaxin 5 was much weaker in cTAGE5 knockdown cells. Quantitation of protein levels is shown in the right panel. All data are means ± SEM (Student's *t* test) from three independent experiments. ***, $P < 0.001$; ns, not significant. (C) Constructs expressing Sec31a, Sec22b, and cTAGE5 were transfected alone or in combination into 293 cells; 24 h later, cell lysates were immunoprecipitated with Flag agarose beads and the immune complexes were detected with indicated antibodies. *, IgG band. (D) Control and cTAGE5 knockdown MIN6 cells stained for Sec22b and Sec31a. Bar, 10 µm. (E) MIN6 cells were incubated with BFA (5 µg/ml) for 1 h at 37°C, washed with PBS, and then fixed and stained with Sec22b, cTAGE5, or Sec31a antibodies. Bar, 10 µm. Ctrl, control.

Sec22b shRNA in MIN6 cells followed by lentivirus-mediated mPro-CpepSfGFP expression. As shown in Fig. 5 A, the level of CpepSfGFP in Sec22b knockdown cells was significantly lower than that in control cells. This result indicates that dysfunction of Sec22b impairs the cleavage of proinsulin, a phenotype recapitulating that observed in cTAGE5 knockdown cells (Fig. 3 E).

cTAGE5 mediates the interaction between components of COPII and SNARE complexes

We have shown that cTAGE5 interacted with Sec22b, which was also reported to interact with t-SNARE Syntaxin5 (Hay, 2001; Jahn and Scheller, 2006). We therefore hypothesized that cTAGE5 might mediate Sec22b-SNARE and Sec22b-COPII transport pathways. To test this postulation, we performed coIP analysis using Sec22b antibody in MIN6 cells. As shown in Fig. 5 B, endogenous cTAGE5, Sec23a, Sec31a, and Syntaxin5 were all detected in the same immunocomplex. More important, the levels of Sec31a and Syntaxin5 coimmunoprecipitated were significantly lower in cTAGE5 knockdown cells. This implicates that components of COPII and SNARE complexes might interact with each other. To further confirm that cTAGE5 played a role in the interaction between components of the two complexes, constructs encoding cTAGE5, Sec31a, and Sec22b were transfected into 293 cells individually or in combination, and coIP experiments were performed. Sec22b was able to interact with Sec31a, and this interaction was enhanced significantly when coexpressed with cTAGE5 (Fig. 5 C). These results indicate that components of COPII and SNARE complexes interact with each other and cTAGE5 is important for the interaction.

Consistent with the coIP results, Sec31a and Sec22b colocalized with each other on ERES, and cTAGE5 depletion disturbed the distribution pattern of Sec22b on ERES (Fig. 5 D). We went on to inspect whether the interaction between cTAGE5 and Sec22b was a dynamic process regulated by the ER-to-Golgi trafficking. MIN6 cells were treated with 5 µg/ml Brefeldin A (BFA) for 1 h to destroy the Golgi apparatus. As expected, Sec22b partially colocalized with ERES markers cTAGE5 and Sec31a in untreated cells. However, cTAGE5 and Sec31a showed a more concentrated pattern at ERES when the Golgi was destroyed by BFA, whereas Sec22b lost much of its localization at ERES (Fig. 5 E). These results indicate that cTAGE5 recruits Sec22b to ERES, and the interaction of Sec22b with cTAGE5 and Sec31a might be regulated by the dynamic transport process.

The coil–coil 2 domain of cTAGE5 interacts with the linker region of Sec22b

We went on to dissect which domain of cTAGE5 was responsible for its interaction with Sec22b. We generated full-length and different deletion mutants of cTAGE5 (Fig. 6 A) and they were transfected into 293 cells individually or in combination, and coIP experiments revealed that the two coil–coil domains in the N-terminal half of cTAGE5 were important for the interaction between cTAGE5 and Sec22b (Fig. 6 B). We further dissected the coil–coil domains into coil–coil 1 and coil–coil 2 domains and found out that the coil–coil 2 domain was more important for the interaction (Fig. 6 C). Vice versa, we also mapped which domain in Sec22b was responsible for its interaction with cTAGE5. We generated full-length and different deletion mutants of Sec22b (Fig. 6 D), and they were transfected into 293 cells individually or in combination, and coIP experiments revealed that Sec22b (120–215) was able to interact with cTAGE5 at a reduced level, compared with Sec22b (100–215). In contrast, Sec22b (134–215) completely lost its ability to bind cTAGE5 (Fig. 6 E). These results indicate that the linker region of Sec22b (120–134 aa) is essential for the interaction between cTAGE5 and Sec22b. In addition, the Sec22b transmembrane domain deletion mutant (Sec22b △TMD) also lost its ability to

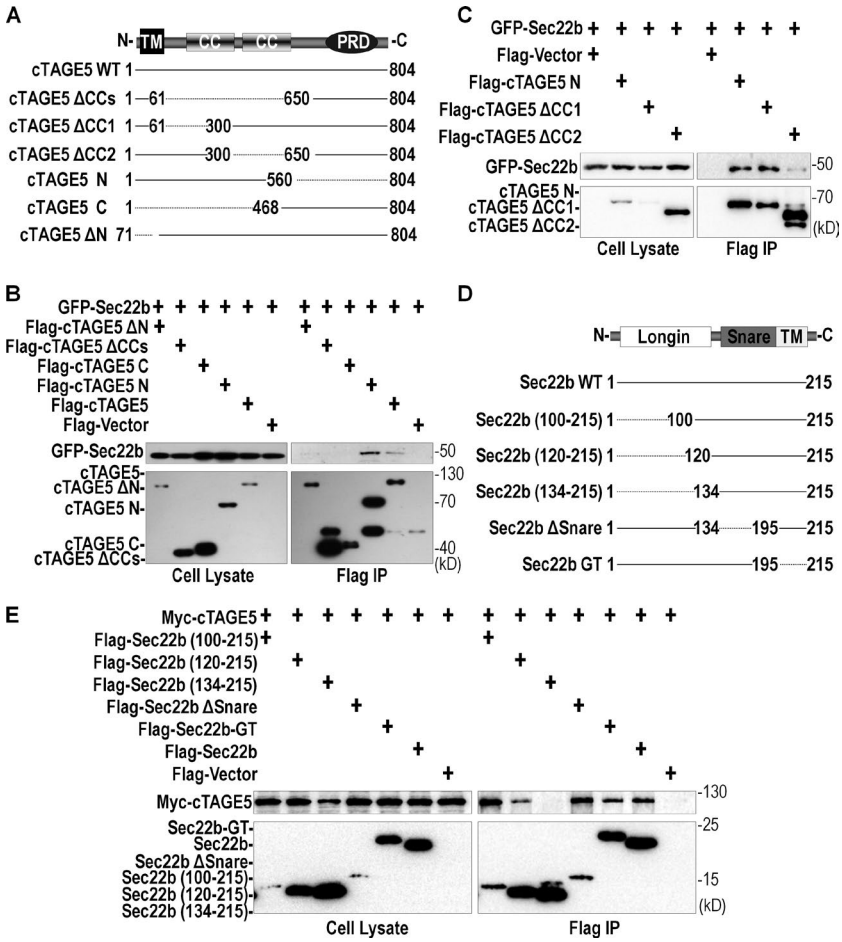

Figure 6. **The coil–coil 2 domain of cTAGE5 interacts with the linker region of Sec22b.** (A) Schematic representation of the cTAGE5 full-length or different deletion mutants. CC, coil–coil domain; PRD, proline-rich domain; TM, transmembrane domain. (B and C) The interaction of Sec22b with cTAGE5 full-length or mutants was analyzed by coIP. Constructs expressing Sec22b and cTAGE5 full-length or mutants were transfected alone or in combination into 293 cells. 24 h later, cell lysates were immunoprecipitated with Flag agarose beads, and the immune complexes were detected with Flag or GFP antibody. (D) Schematic representation of the Sec22b full-length or different deletion mutant. Sec22b GT is the swap of TM of Sec22b (195–215 aa) with that of GOSR2 (191–211 aa). (E) The interaction of cTAGE5 with Sec22b full-length or mutants was assessed by coIP as in B.

interact with cTAGE5 (Fig. S4 F). To prove that this was a result of the disruption of the membrane binding ability, we restored its membrane binding ability by domain swap with a GOSR2 TM domain (Sec22b GT) and found that the interaction with cTAGE5 was restored (Fig. 6 E).

The interaction between cTAGE5 and Sec22b is essential for proinsulin trafficking

To test the function of the interaction between cTAGE5 and Sec22b, we inspected whether or not deletion of the coil–coil 2 domain of cTAGE5 could rescue the proinsulin cleavage defect. cTAGE5 knockdown MIN6 cells were infected with lentivirus carrying a full-length human *cTAGE5* (h*cTAGE5*) cDNA, coil–coil 1 domain or coil–coil 2 domain deletion mutants, respectively. The expression of hcTAGE5 full-length or mutants was detected by Western blotting with cTAGE5 and Flag antibody (Fig. 7 A). Importantly, the levels of CpepSfGFP cleaved from the mPro-CpepSfGFP increased very significantly with expression of full-length or coil–coil 1 domain deletion mutant, but not with coil–coil 2 domain deletion mutant of hcTAGE5 (Fig. 7 A). Consistent with this result, full-length hcTAGE5 and coil–coil 1 domain deletion mutant, but not the coil–coil 2 domain deletion mutant, colocalized with Sec31a (Fig. S5 A). Furthermore, in cTAGE5 knockdown MIN6 cells, the distribution pattern of Sec22b could be rescued by full-length or coil–coil 1 domain deletion mutant, as illustrated by much more localization at ERES (Fig. S5 B). In contrast, it could not be rescued by the expression of the coil–coil 2 domain deletion mutant. Collectively, the results indicate that the interaction between Sec22b and cTAGE5 is important for the distribution of Sec22b and proinsulin trafficking from ER to Golgi.

More important, we generated a transgenic mouse line with h*cTAGE5* cDNA inserted into ROSA26 loci (Fig. S5 C). Through immunostaining, we detected the expression of hcTAGE5 protein specifically in β cells and observed largely normal islet architecture in the *cTAGE5* cKO background (Fig. 7, B and C). Consistent with the results from the in vitro experiment, *hcTAGE5* transgenic mice on the *cTAGE5* cKO background exhibited normal glucose tolerance (Fig. 7 D). These results indicate that both the islet structure and insulin biogenesis defect in cKO mice could be rescued by hcTAGE5.

Discussion

cTAGE5/MEA6 has been shown to interact with COPII components to regulate the secretion of mega cargos, VLDL, and collagen VII (Santos et al., 2016; Wang et al., 2016). In this study, we provide evidence that cTAGE5 is also required for the secretion of small molecules. Ablation of *cTAGE5* specifically in pancreatic β cells leads to impaired glucose-stimulated insulin secretion and subsequently glucose intolerance, as a result of the defect in the transport of proinsulin from ER to Golgi. cTAGE5 interacts with Sec22b, and they are likely to be involved in the release of COPII vesicle or the formation of the preGolgi intermediate compartment for proinsulin trafficking (Fig. 8).

The glucose intolerance in *cTAGE5* cKO islets is caused by the significantly reduced insulin secretion caused by the dimin-

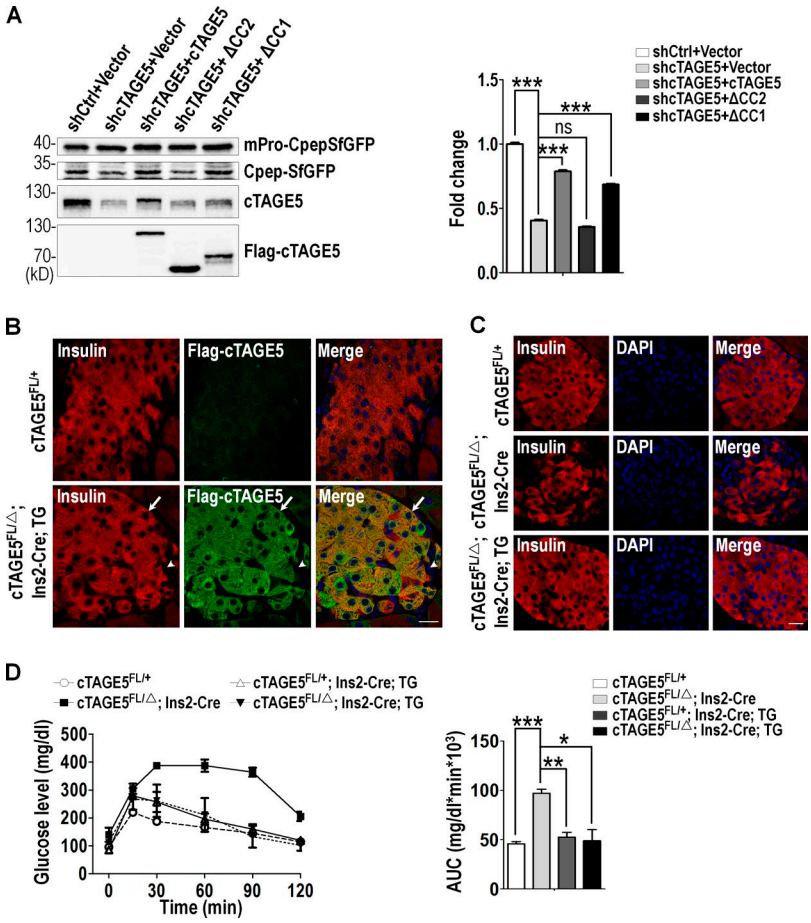

Figure 7. **The interaction between cTAGE5 and Sec22b is important for proinsulin processing.** (A) MIN6 cells were infected with lentivirus expressing scramble (shCtrl) or shcTAGE5, together with lentivirus expressing vector, human cTAGE5 full-length, or mutants (cTAGE5 △CC1 and cTAGE5 △CC2). Proinsulin processing was analyzed as in Fig. 5 A. (B) Pancreas sections stained with insulin (red) and Flag-cTAGE5 (green). The arrow shows β cell in islets; the arrowhead shows non–β cells in islets. TG, h*cTAGE5* transgenic mice. Bar, 50 µm. (C) Pancreas sections stained with insulin (red) and DAPI (blue). Bar, 50 µm. (D) IPGTT was performed. Area under the curve (AUC) shown at right (n = 3 for all mouse lines). All data are means ± SEM (Student's t test) from more than two independent experiments. *, P < 0.05; **, P < 0.01; ***, P < 0.001; ns, not significant.

ished mature insulin content in the pancreas (Fig. 1). Considering the role of cTAGE5 in cargo transportation, we postulate that reduced insulin biogenesis might be caused by a defect of proinsulin transport from ER to Golgi. The increased detention of proinsulin in ER and reduced distribution of proinsulin in ERGIC53 and Golgi in *cTAGE5* cKO β cells support this speculation (Fig. 3, A–C). In addition, we adopted a reporter for ER-to-Golgi transport and found that proinsulin transport declines significantly in cTAGE5 knockdown cells (Fig. 3, E and F). Furthermore, proinsulin biosynthesis accounts for 50% of total protein synthesis in stimulated β cells. In the case of a defect in ER-to-Golgi transport, proinsulin would accumulate in ER and be misfolded, which eventually results in ER stress (Riahi et al., 2016). Indeed, the increase of ER stress and the significantly increased binding of unfolded proinsulin with Bip are detected in *cTAGE5* cKO islets (Fig. 3 D). Therefore, deletion of *cTAGE5* in β cells affects the proinsulin transport from the ER to the Golgi, which leads to the reduced levels of mature insulin, as well as ER stress and reduced islet sizes. The reduced islet mass in the cKO pancreas may account for only part of the decreased insulin level, because the levels of proinsulin are largely normal (Fig. S3, A and B).

ER stress is well known to be capable of causing apoptosis. Deletion of *cTAGE5* leads to increased apoptosis and decreased islet mass in the cKO pancreas (Fig. 2). In addition to increased ER stress, we notice a significant decrease in Akt activity. It will be intriguing to study in the future whether the increased ER stress and reduced insulin signaling, which is involved in the Akt pathway, affect β cell survival sequentially or synergistically in the *cTAGE5* cKO pancreas.

SNARE proteins have been shown to enable the docking and fusing of COPII vesicles with Golgi and participate in ER-to-Golgi transport (Lee et al., 2004; Chatre et al., 2005; Petkovic et al., 2014). In the present study, we show that cTAGE5 interacts with Sec22b mainly through the coil–coil 2 domain of cTAGE5 and the linker region of Sec22b (Fig. 6). In addition, the interaction between cTAGE5 and Sec22b is essential for proinsulin cleavage (ER-to-Golgi transport; Fig. 7 A). Furthermore, the distribution of Sec22b is specifically altered in *cTAGE5* cKO β cells, suggesting that cTAGE5 is important for the circulation of Sec22b between the ER and Golgi (Fig. 4). More important, knockdown of Sec22b also impairs proinsulin cleavage, indicating that Sec22b is essential for proinsulin trafficking (Fig. 5 A). The linker region of the SNARE family is important for SNARE complex formation (Wang et al., 2017). The Longin domain usually binds to the SNARE domain when it resides in ER, and the Longin domain unfolds from the SNARE domain when it travels to Golgi and facilitates the SNARE domain to interact with t-SNARE. Thus, we propose that when it is in its folding conformation, the linker region interacts with cTAGE5. The interaction of Sec22b with both COPII and t-SNARE components (Fig. 5 B) indicates that this interaction might be dynamically regulated by the transport process. This is confirmed when the transport pathway is disrupted by BFA treatment (Fig. 5 E). Therefore, cTAGE5 may coordinate with Sec22b in the release of COPII vesicle from ER and the formation of the preGolgi intermediate compartment (Fig. 8).

cTAGE5 has been shown to interact and coordinate with TANGO1 to play a role in the megacargo secretion pathway

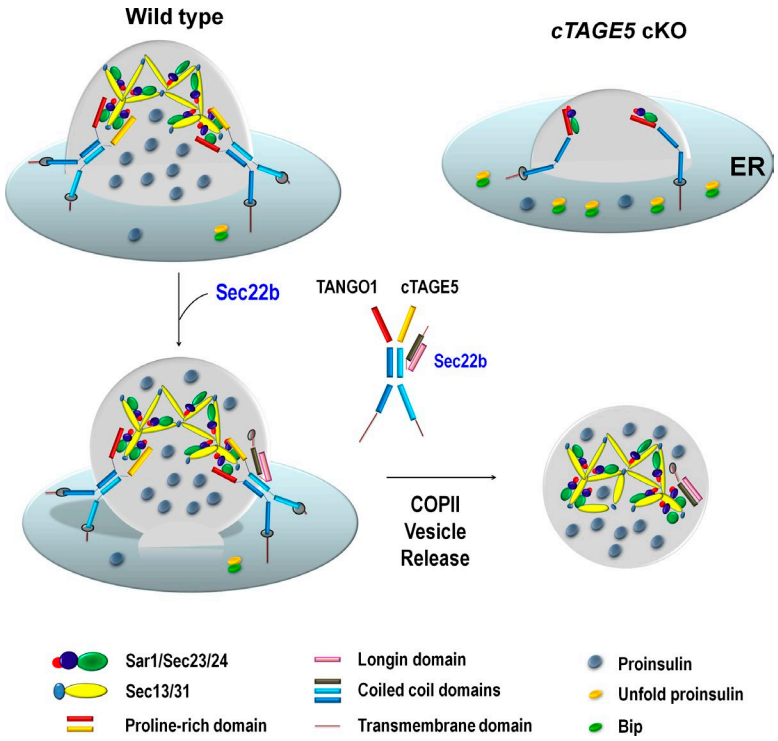

Figure 8. **Scheme for the role of cTAGE5 and Sec22b in the ER-to-Golgi trafficking of proinsulin.** cTAGE5 and TANGO1 can form a heterodimer to regulate the formation of COPII vesicle containing proinsulin on the ERES. Sec22b can interact with cTAGE5, and they are likely to coordinate with each other in the release of COPII vesicle and the formation of preGolgi intermediate compartment, and thereby the ER-to-Golgi trafficking of proinsulin.

(Saito et al., 2011). *Tango1* knockout mice die after birth, but *cTAGE5* knockout mice die at embryonic day 8.5 to 9.5 (Wilson et al., 2011; Wang et al., 2016). This indicates that cTAGE5 and TANGO1 may play some nonoverlapping roles, at least, during embryo development. We provide evidence here that cTAGE5 is indispensable for the trafficking of proinsulin, which has a molecular weight of only ∼9 kD. Our study therefore sheds light on the more profound role of cTAGE5 in the transport of both big and small cargoes.

cTAGE5 has been indicated as a shorter spliced variant of TALI, a TANGO1-like protein with similar domains (Santos et al., 2016), and the protein level of TALI was also reduced in *cTAGE5* cKO islets (Fig. S5 D). We show here that expression of human cTAGE5 can rescue the proinsulin processing defect in cTAGE5 knockdown cells and, more important, transgenic expression of human cTAGE5 specifically in β cells is able to rescue the defect in islet structure and insulin biogenesis, as well as reversing glucose intolerance on the *cTAGE5* cKO background (Fig. 7). Therefore, cTAGE5 is likely to play a role in insulin secretion independent of TALI.

In summary, we show in this study that ablation of *cTAGE5* in pancreatic β cells leads to serious defects in insulin production with resultant chronic hyperglycemia and glucose intolerance in mice. We provide evidence that cTAGE5 interacts with a v-SNARE protein, Sec22b, to regulate the transport of proinsulin from ER to Golgi. These findings provide insights not only into mechanisms underlying the basic cellular process of ER-to-Golgi trafficking but also for our understanding of the pathogenesis of diabetes and related conditions.

Materials and methods

Generation of *cTAGE5* knockout and transgenic mice

cTAGE5$^{\Delta/+}$ and *cTAGE5*$^{Flox/Flox}$ mice were previously generated (Wang et al., 2016). *cTAGE5* was specifically deleted in pancreatic β cells by crossing *cTAGE5*$^{\Delta/+}$*; Insulin2 (Ins2)-Cre* with *cTAGE5*$^{FL/FL}$ mice, which would generate four different lines (i.e., *cTAGE5*$^{FL/\Delta}$*; Ins2-Cre*, *cTAGE5*$^{FL/+}$*; Ins2-Cre*, *cTAGE5*$^{FL/+}$, and *cTAGE5*$^{FL/\Delta}$). To generate *cTAGE5* transgenic mice, a human *cTAGE5* cDNA driven by CAG promoter followed by a stop codon flanked by two LoxP sites was inserted into the first intron of Rosa26 allele through CRISPR/Cas9 technology (Fig. S5 C). This model was generated by Beijing Biocytogen Co., Ltd. All mice were in a 129/SvEv and C57BL/6 mixed background. Tail biopsies were used to extract genomic DNA for genotyping. All experimental procedures were performed according to protocols approved by the Institutional Animal Care and Use Committee at the Institute of Genetics and Developmental Biology, Chinese Academy of Sciences.

Intraperitoneal glucose and insulin tolerance tests

IPGTT assays were performed 16 h after fast with free access to water and then injected i.p. with D-glucose at 2 mg/g of body weight. Plasma insulin levels were measured using a mouse ultrasensitive insulin ELISA kit (ALPCO). IPITT assays were performed 6 h after fast with free access to water and then injected with human insulin (Novolin) at 0.75 units/kg of body weight. Blood glucose levels were assessed at the indicated times.

Islet isolation and glucose-stimulated insulin secretion

Mouse islets were isolated after injecting collagenase XI (C7657; Sigma-Aldrich) into the pancreas through the common bile duct as previously described (Li et al., 2009). Then the distended pancreas was removed and digested in a 37°C water bath for 15 min. After incubation, the pancreas was disrupted into homogenous suspension and filtered through a 300-µm cell strainer. Finally, islets were picked up under a microscope. Glucose-stimulated insulin secretion was measured by static incubation of isolated islets. After overnight culture in RPMI-1640 medium, groups of 20 islets of approximately the same size were first equilibrated with Krebs Ringer buffer (KRB; 128 mM NaCl, 4.8 mM KCl, 1.2 mM KH_2PO_4, 1.2 mM $MgSO_4$, 2.5 mM $CaCl_2$, 5 mM $NaHCO_3$, 10 mM Hepes, and 0.1% BSA) containing 2.8 mM glucose for 30 min at 37°C. Then islets were incubated in KRB containing 2.8 mM glucose for 1 h at 37°C. After the supernatant was collected,

islets were stimulated with KRB containing 16.7 mM glucose for another 1 h at 37°C. Total insulin content of islets was harvested by overnight extraction in acid ethanol. Secreted insulin in supernatant was measured by mouse ultrasensitive insulin ELISA kit (ALPCO).

Genotyping PCR and real-time PCR

The genotypes of mice were detected by PCR as previously described (Zhang et al., 2014; Wang et al., 2016). Total RNA was extracted from isolated islets using TRIzol reagent (Invitrogen). Real-time PCR was performed according to the protocol of the manufacturer. The primers for real-time PCR are listed in Table S1.

TEM

The procedures of TEM were described as previously (Wang et al., 2016; Zhang et al., 2016). Concisely, isolated islets were fixed with 2.5% glutaraldehyde, postfixed in 1% osmium tetroxide, dehydrated in acetone, and then embedded in EPON812 resin. Ultrathin sections were mounted on copper grids and photographed for TEM. The density of secretory granules in β cells was measured by ImageJ software.

Immunostaining, H&E staining, and islet number measurement

Pancreases were fixed with 4% paraformaldehyde, dehydrated in graded ethanol series, and embedded in paraffin. Sections of 5-µm thickness were prepared by a rotary microtome (RM2255; Leica) and used for immunostaining after deparaffinization. MIN6 cells cultured on coverslips were fixed in cold methanol for 15 min at −20°C, permeabilized with 0.3% Triton/PBS for 10 min, blocked with 5% BSA for 1 h, and incubated overnight with primary antibody. The following antibodies were used for immunostaining: Insulin (1:100; ab7842; Abcam); Glucagon (1:100; G2654; Sigma-Aldrich); Ki67 (1:1,000; ab15580; Abcam); cTAGE5 (1:200; HPA000387; Sigma-Aldrich); Proinsulin (1:500; 2PR8; Hytest); Sec22b (1:100; sc-101267; Santa Cruz Biotechnology); Calnexin (1:250; MA3-027; ThermoFisher); LMAN1 (1:200; ab125006; Abcam); GM130 (1:200; ab52649; Abcam); and Vamp2 (1:200; ab181869; Abcam). The secondary antibodies conjugated with Alexa Fluor 488, 568, or 647 were purchased from Invitrogen, and those conjugated with HRP using DAB as chromogen from Cwbio. Sections were photographed by an LSM 700 (Carl Zeiss) confocal microscope equipped with a 40× water immersion objective (1.0 NA) or 100× oil immersion objective (1.4 NA) at room temperature and analyzed with ImageJ or Imaris software.

For islet number measurements, three serial sections of 5 µm were obtained from each pancreas at 100-µm intervals. All sections were processed for H&E staining, and the images were acquired by an eclipse TE2000-S (Nikon) equipped with a 4× 0.13 NA objective and a DXM 1200C camera. The islet number per unit area was calculated in a random way.

Cell culture, transfection, Western blotting, and coIP

A total of 293 cells were cultured in DMEM (Hyclone) supplemented with 10% FBS (Excell), and 293 cells were transiently transfected with Vigofect (Vigorous). MIN6 cells were cultured in DMEM (Gibco) supplemented with 10% FBS, 50 µM 2-mercaptoethanol. Plasmids were transiently transfected into MIN6 cells with Lipo2000 (Invitrogen). The GFP-Sec22b plasmid was a gift from T. Galli (INSERM, Paris, France). The COPII constructs were gifts from S. Yu (Chinese University of Hong Kong, Hong Kong, China). Western blotting and coIP were described previously (Xu et al., 2003, 2014; Yang et al., 2012). In brief, cells were lysed with cell lysis buffer consisting of 50 mM Tris-HCl, pH 7.4, 100 mM NaCl, 2 mM EDTA, 1% NP-40, and protease inhibitors, and centrifuged at 12,000 rpm for 10 min at 4°C. Cell lysates were collected and immunoprecipitated with Flag M2 beads (A2220; Sigma-Aldrich). The beads were washed five times, and bound proteins were eluted from beads with 2× SDS sample buffer. The following antibodies were used for Western blotting: α-tubulin (1:3,000; 3873s; CST); Bip (1:10,000; ab21685; Abcam); PDI (1:1,000; ab2792; Abcam); Caspase3 (1:1,000; ab13847; Abcam); P-Akt (1:1,000; 9018; CST); Akt (1:1,000; 1085; Epitomics); GAPDH (1:2,000; 2118s; CST); Sec24d (1:1,000; ab191566; Abcam); P115 (1:1,000; 13509-1-AP; Proteintech); Sec13 (1:1,000; ab168824; Abcam); Sec31a (1:1,000; 13466; CST); Sec23a (1:1,000; 8162; CST); Syntaxin5 (1:1,000; sc-365124; Santa Cruz Biotechnology); Flag (1:3,000; M185; MBL); Myc (1:1,000; M562; MBL); HA (1:3,000; M180; MBL); GFP (1:2,000; sc-9996; Santa Cruz Biotechnology); GFP (1:5,000; ab290; Abcam); and Calnexin (1:5,000; GTX109669; GeneTex).

Lentivirus shRNA knockdown of cTAGE5 and Sec22b

The following shRNAs were purchased from YILE Biotech: cTAGE5 (target sequence 5′-CCGGCAAGTGAATGATCTCGATAAACT CGAGTTTATCGAGATCATTCACTTGTTTTTG-3′); Sec22b (target sequence 5-′CCGGGCATTGGATTCAAAGGCTAACCTCGA GGTTAGCCTTTGAATCCAATGCTTTTTG-3′); and the negative control (target sequence 5′-CCGGCAACAAGATGAAGAGCACCA ACTCGAGTTGGTGCTCTTCATCTTGTTGTTTTTG-3′). The lentiviruses expressing shRNA were produced with a four-plasmid system following the manufacturer's instructions. For establishment of cTAGE5 knockdown cell line or Sec22b knockdown cell line, MIN6 cells were cultured in a 24-well plate and infected with lentivirus. Then the cells were transferred to a 6-cm dish at 80–90% confluence and treated with puromycin (4 µg/ml, Millipore) for several passages until almost all of the cells were infected with lentivirus. After that, the stable cell line was maintained with 2 µg/ml puromycin.

Construction of mPro-CpepSfGFP

The plasmid of superfolder GFP was purchased from Addgene, and construction of mPro-CpepSfGFP was performed as described previously (Liu et al., 2007; Haataja et al., 2013). In brief, the mouse preproinsulin was amplified by PCR and subcloned into pcDNA3.1 vector. For generating the mPro-CpepSfGFP construct, the superfolder GFP sequence was inserted into the mouse preproinsulin C-peptide sequence through the BstEII site. The sequence of mPro-CpepSfGFP was confirmed by direct DNA sequencing.

Subcellular fractionation

Subcellular fractionation was performed as previously described (de Araùjo et al., 2008; Li et al., 2012). In brief, two 10-cm dishes of MIN6 cells were washed three times with ice-cold PBS and scraped in 2 ml ice-cold PBS with 0.5× protease inhibitors. Cells were homogenized in 500 µl homogenization buffer plus (250 mM sucrose, 1 mM EDTA, 0.03 mM cycloheximide, 3 mM imidazole, pH 7.4, and protease inhibitors) with a 1-ml syringe attached to a 22-G needle, and then centrifuged at 2,000 *g* for 10 min to remove nuclear debris and unbroken cells. The postnuclear supernatant was carefully retrieved and floated on top of 10–45% continuous sucrose gradient in a SW41 tube. The samples were centrifuged at 210,000 *g* for 18 h at 4°C. Fractions were collected and concentrated by TCA precipitation for Western blotting analysis.

Statistical analysis

All statistical analyses were acquired from more than two independent experiments, values were expressed as means ± SEM, and two-sample comparisons were performed using an unpaired Student's *t* test. *, $P < 0.05$ was considered statistical significance. For the *t* test, data distribution was assumed to be normal, but this was not formally tested. All statistical analyses were presented using Prism software (GraphPad Software, Inc.).

Online supplemental material

Fig. S1 shows sex and age do not affect the phenotype. Fig. S2 shows hyperglycemia is observed only in *cTAGE5$^{FL/\Delta}$; Ins2-Cre* mice. Fig. S3 shows the proinsulin levels, genes involved in exocytosis, and β cell proliferation are unchanged in cKO islets. Fig. S4 shows deletion of *cTAGE5* in the liver leads to ER stress, and cTAGE5 and Sec22b do not affect each other's expression. Fig. S5 shows the cellular location of cTAGE5 full-length or mutant proteins and Sec22b in cTAGE5 knockdown MIN6 cells.

Acknowledgments

We would like to thank Dr. T. Galli for providing GFP-Sec22b construct, Dr. Sidney Yu for providing COPII constructs, Dr. John Speakman for editing the paper, Drs. Xiaowei Chen and Xun Huang for their valuable advice, and Dr. Lin Yang for her help with TEM.

This work was supported in part by grants from the National Science Foundation of China (31771569/31471132/31430037/31571038/31730108) and Chinese Academy of Sciences (QYZDJ-SSW-SMC007/GJHZ1827).

The authors declare no competing financial interests.

Author contributions: J. Fan, Y. Wang, and Z. Xu designed the project, analyzed the data, and wrote the manuscript. L. Liu and M. Yu made the WT cTAGE5 and the mutants. H. Zhang and F. Zhang performed some data analysis. L. Shi and F. Gao provided the resources. Z. Xu is the guarantor of this work.

Submitted: 6 May 2017
Revised: 31 July 2017
Accepted: 8 September 2017

References

Adolf, F., M. Rhiel, I. Reckmann, and F.T. Wieland. 2016. Sec24C/D-isoform-specific sorting of the preassembled ER-Golgi Q-SNARE complex. *Mol. Biol. Cell.* 27:2697–2707. https://doi.org/10.1091/mbc.E16-04-0229

Ashcroft, F.M., and P. Rorsman. 2012. Diabetes mellitus and the β cell: the last ten years. *Cell.* 148:1160–1171. https://doi.org/10.1016/j.cell.2012.02.010

Bentley, M., Y. Liang, K. Mullen, D. Xu, E. Sztul, and J.C. Hay. 2006. SNARE status regulates tether recruitment and function in homotypic COPII vesicle fusion. *J. Biol. Chem.* 281:38825–38833. https://doi.org/10.1074/jbc.M606044200

Chatre, L., F. Brandizzi, A. Hocquellet, C. Hawes, and P. Moreau. 2005. Sec22 and Memb11 are v-SNAREs of the anterograde endoplasmic reticulum-Golgi pathway in tobacco leaf epidermal cells. *Plant Physiol.* 139:1244–1254. https://doi.org/10.1104/pp.105.067447

Comtesse, N., I. Niedermayer, B. Glass, D. Heckel, E. Maldener, W. Nastainczyk, W. Feiden, and E. Meese. 2002. MGEA6 is tumor-specific overexpressed and frequently recognized by patient-serum antibodies. *Oncogene.* 21:239–247. https://doi.org/10.1038/sj.onc.1205005

de Araùjo, M.E., L.A. Huber, and T. Stasyk. 2008. Isolation of endocitic organelles by density gradient centrifugation. *Methods Mol. Biol.* 424:317–331. https://doi.org/10.1007/978-1-60327-064-9_25

Fang, J., M. Liu, X. Zhang, T. Sakamoto, D.J. Taatjes, B.P. Jena, F. Sun, J. Woods, T. Bryson, A. Kowluru, et al. 2015. COPII-Dependent ER Export: A Critical Component of Insulin Biogenesis and β-Cell ER Homeostasis. *Mol. Endocrinol.* 29:1156–1169. https://doi.org/10.1210/me.2015-1012

Gething, M.J., and J. Sambrook. 1992. Protein folding in the cell. *Nature.* 355:33–45. https://doi.org/10.1038/355033a0

Gonzalez, L.C. Jr., W.I. Weis, and R.H. Scheller. 2001. A novel snare N-terminal domain revealed by the crystal structure of Sec22b. *J. Biol. Chem.* 276:24203–24211. https://doi.org/10.1074/jbc.M101584200

Gupta, S., B. McGrath, and D.R. Cavener. 2010. PERK (EIF2AK3) regulates proinsulin trafficking and quality control in the secretory pathway. *Diabetes.* 59:1937–1947. https://doi.org/10.2337/db09-1064

Haataja, L., E. Snapp, J. Wright, M. Liu, A.B. Hardy, M.B. Wheeler, M.L. Markwardt, M. Rizzo, and P. Arvan. 2013. Proinsulin intermolecular interactions during secretory trafficking in pancreatic β cells. *J. Biol. Chem.* 288:1896–1906. https://doi.org/10.1074/jbc.M112.420018

Hasegawa, Y., Y. Daitoku, S. Mizuno, Y. Tanimoto, S. Mizuno-Iijima, M. Matsuo, N. Kajiwara, M. Ema, H. Oishi, Y. Miwa, et al. 2014. Generation and characterization of Ins1-cre-driver C57BL/6N for exclusive pancreatic beta cell-specific Cre-loxP recombination. *Exp. Anim.* 63:183–191. https://doi.org/10.1538/expanim.63.183

Hay, J.C. 2001. SNARE complex structure and function. *Exp. Cell Res.* 271:10–21. https://doi.org/10.1006/excr.2001.5368

Heit, J.J., S.K. Karnik, and S.K. Kim. 2006. Intrinsic regulators of pancreatic beta-cell proliferation. *Annu. Rev. Cell Dev. Biol.* 22:311–338. https://doi.org/10.1146/annurev.cellbio.22.010305.104425

Jahn, R., and R.H. Scheller. 2006. SNAREs--engines for membrane fusion. *Nat. Rev. Mol. Cell Biol.* 7:631–643. https://doi.org/10.1038/nrm2002

Joglekar, A.P., and J.C. Hay. 2005. Evidence for regulation of ER/Golgi SNARE complex formation by hsc70 chaperones. *Eur. J. Cell Biol.* 84:529–542. https://doi.org/10.1016/j.ejcb.2004.12.028

Kusminski, C.M., S. Shetty, L. Orci, R.H. Unger, and P.E. Scherer. 2009. Diabetes and apoptosis: lipotoxicity. *Apoptosis.* 14:1484–1495. https://doi.org/10.1007/s10495-009-0352-8

Lee, M.C., E.A. Miller, J. Goldberg, L. Orci, and R. Schekman. 2004. Bi-directional protein transport between the ER and Golgi. *Annu. Rev. Cell Dev. Biol.* 20:87–123. https://doi.org/10.1146/annurev.cellbio.20.010403.105307

Li, D.S., Y.H. Yuan, H.J. Tu, Q.L. Liang, and L.J. Dai. 2009. A protocol for islet isolation from mouse pancreas. *Nat. Protoc.* 4:1649–1652. https://doi.org/10.1038/nprot.2009.150

Li, H., S. Wei, K. Cheng, N.V. Gounko, R.E. Ericksen, A. Xu, W. Hong, and W. Han. 2014. BIG3 inhibits insulin granule biogenesis and insulin secretion. *EMBO Rep.* 15:714–722.

Li, X., J. Ye, L. Zhou, W. Gu, E.A. Fisher, and P. Li. 2012. Opposing roles of cell death-inducing DFF45-like effector B and perilipin 2 in controlling hepatic VLDL lipidation. *J. Lipid Res.* 53:1877–1889. https://doi.org/10.1194/jlr.M026591

Lindahl, M., T. Danilova, E. Palm, P. Lindholm, V. Võikar, E. Hakonen, J. Ustinov, J.O. Andressoo, B.K. Harvey, T. Otonkoski, et al. 2014. MANF is indispensable for the proliferation and survival of pancreatic β cells. *Cell Reports.* 7:366–375. https://doi.org/10.1016/j.celrep.2014.03.023

Liu, M., I. Hodish, C.J. Rhodes, and P. Arvan. 2007. Proinsulin maturation, misfolding, and proteotoxicity. *Proc. Natl. Acad. Sci. USA.* 104:15841–15846. https://doi.org/10.1073/pnas.0702697104

Liu, M., J. Wright, H. Guo, Y. Xiong, and P. Arvan. 2014. Proinsulin entry and transit through the endoplasmic reticulum in pancreatic beta cells. *Vitam. Horm.* 95:35–62. https://doi.org/10.1016/B978-0-12-800174-5.00002-8

Mancias, J.D., and J. Goldberg. 2007. The transport signal on Sec22 for packaging into COPII-coated vesicles is a conformational epitope. *Mol. Cell.* 26:403–414. https://doi.org/10.1016/j.molcel.2007.03.017

Morley, T.S., J.Y. Xia, and P.E. Scherer. 2015. Selective enhancement of insulin sensitivity in the mature adipocyte is sufficient for systemic metabolic improvements. *Nat. Commun.* 6:7906. https://doi.org/10.1038/ncomms8906

Petkovic, M., A. Jemaiel, F. Daste, C.G. Specht, I. Izeddin, D. Vorkel, J.M. Verbavatz, X. Darzacq, A. Triller, K.H. Pfenninger, et al. 2014. The SNARE Sec22b has a non-fusogenic function in plasma membrane expansion. *Nat. Cell Biol.* 16:434–444. https://doi.org/10.1038/ncb2937

Riahi, Y., J.D. Wikstrom, E. Bachar-Wikstrom, N. Polin, H. Zucker, M.S. Lee, W. Quan, L. Haataja, M. Liu, P. Arvan, et al. 2016. Autophagy is a major regulator of beta cell insulin homeostasis. *Diabetologia.* 59:1480–1491. https://doi.org/10.1007/s00125-016-3868-9

Saito, K., K. Yamashiro, Y. Ichikawa, P. Erlmann, K. Kontani, V. Malhotra, and T. Katada. 2011. cTAGE5 mediates collagen secretion through interaction with TANGO1 at endoplasmic reticulum exit sites. *Mol. Biol. Cell.* 22:2301–2308. https://doi.org/10.1091/mbc.E11-02-0143

Saito, K., K. Yamashiro, N. Shimazu, T. Tanabe, K. Kontani, and T. Katada. 2014. Concentration of Sec12 at ER exit sites via interaction with cTAGE5 is required for collagen export. *J. Cell Biol.* 206:751–762. https://doi.org/10.1083/jcb.201312062

Saliminejad, K., F. Ashtari, K. Kamali, H. Edalatkhah, and H.R. Khorram Khorshid. 2013. Analysis of the CTAGE5 P521A variation with the risk of familial idiopathic basal ganglia calcification in an Iranian population. *J. Mol. Neurosci.* 49:614–617. https://doi.org/10.1007/s12031-012-9898-y

Santos, A.J., C. Nogueira, M. Ortega-Bellido, and V. Malhotra. 2016. TANGO1 and Mia2/cTAGE5 (TALI) cooperate to export bulky pre-chylomicrons/VLDLs from the endoplasmic reticulum. *J. Cell Biol.* 213:343–354. https://doi.org/10.1083/jcb.201603072

Scheuner, D., D. Vander Mierde, B. Song, D. Flamez, J.W. Creemers, K. Tsukamoto, M. Ribick, F.C. Schuit, and R.J. Kaufman. 2005. Control of mRNA translation preserves endoplasmic reticulum function in beta cells and maintains glucose homeostasis. *Nat. Med.* 11:757–764. https://doi.org/10.1038/nm1259

Sun, J., J. Cui, Q. He, Z. Chen, P. Arvan, and M. Liu. 2015. Proinsulin misfolding and endoplasmic reticulum stress during the development and progression of diabetes. *Mol. Aspects Med.* 42:105–118. https://doi.org/10.1016/j.mam.2015.01.001

Tang, T., M.J. Abbott, M. Ahmadian, A.B. Lopes, Y. Wang, and H.S. Sul. 2013. Desnutrin/ATGL activates PPARδ to promote mitochondrial function for insulin secretion in islet β cells. *Cell Metab.* 18:883–895. https://doi.org/10.1016/j.cmet.2013.10.012

Usener, D., D. Schadendorf, J. Koch, S. Dübel, and S. Eichmüller. 2003. cTAGE: a cutaneous T cell lymphoma associated antigen family with tumor-specific splicing. *J. Invest. Dermatol.* 121:198–206. https://doi.org/10.1046/j.1523-1747.2003.12318.x

Wang, S., U.B. Choi, J. Gong, X. Yang, Y. Li, A.L. Wang, X. Yang, A.T. Brunger, and C. Ma. 2017. Conformational change of syntaxin linker region induced by Munc13s initiates SNARE complex formation in synaptic exocytosis. *EMBO J.* 36:816–829. https://doi.org/10.15252/embj.201695775

Wang, T., R. Grabski, E. Sztul, and J.C. Hay. 2015. p115-SNARE interactions: a dynamic cycle of p115 binding monomeric SNARE motifs and releasing assembled bundles. *Traffic.* 16:148–171. https://doi.org/10.1111/tra.12242

Wang, Y., L. Liu, H. Zhang, J. Fan, F. Zhang, M. Yu, L. Shi, L. Yang, S.M. Lam, H. Wang, et al. 2016. Mea6 controls VLDL transport through the coordinated regulation of COPII assembly. *Cell Res.* 26:787–804. https://doi.org/10.1038/cr.2016.75

Wickner, W., and R. Schekman. 2008. Membrane fusion. *Nat. Struct. Mol. Biol.* 15:658–664. https://doi.org/10.1038/nsmb.1451

Wijesekara, N., F.F. Dai, A.B. Hardy, P.R. Giglou, A. Bhattacharjee, V. Koshkin, F. Chimienti, H.Y. Gaisano, G.A. Rutter, and M.B. Wheeler. 2010. Beta cell-specific Znt8 deletion in mice causes marked defects in insulin processing, crystallisation and secretion. *Diabetologia.* 53:1656–1668. https://doi.org/10.1007/s00125-010-1733-9

Wilson, D.G., K. Phamluong, L. Li, M. Sun, T.C. Cao, P.S. Liu, Z. Modrusan, W.N. Sandoval, L. Rangell, R.A. Carano, et al. 2011. Global defects in collagen secretion in a Mia3/TANGO1 knockout mouse. *J. Cell Biol.* 193:935–951. https://doi.org/10.1083/jcb.201007162

Xu, D., and J.C. Hay. 2004. Reconstitution of COPII vesicle fusion to generate a pre-Golgi intermediate compartment. *J. Cell Biol.* 167:997–1003. https://doi.org/10.1083/jcb.200408135

Xu, D., A.P. Joglekar, A.L. Williams, and J.C. Hay. 2000. Subunit structure of a mammalian ER/Golgi SNARE complex. *J. Biol. Chem.* 275:39631–39639. https://doi.org/10.1074/jbc.M007684200

Xu, D., F. Zhang, Y. Wang, Y. Sun, and Z. Xu. 2014. Microcephaly-associated protein WDR62 regulates neurogenesis through JNK1 in the developing neocortex. *Cell Reports.* 6:104–116. https://doi.org/10.1016/j.celrep.2013.12.016

Xu, Z., N.V. Kukekov, and L.A. Greene. 2003. POSH acts as a scaffold for a multiprotein complex that mediates JNK activation in apoptosis. *EMBO J.* 22:252–261. https://doi.org/10.1093/emboj/cdg021

Yang, T., Y. Sun, F. Zhang, Y. Zhu, L. Shi, H. Li, and Z. Xu. 2012. POSH localizes activated Rac1 to control the formation of cytoplasmic dilation of the leading process and neuronal migration. *Cell Reports.* 2:640–651. https://doi.org/10.1016/j.celrep.2012.08.007

Ye, R., W.L. Holland, R. Gordillo, M. Wang, Q.A. Wang, M. Shao, T.S. Morley, R.K. Gupta, A. Stahl, and P.E. Scherer. 2014. Adiponectin is essential for lipid homeostasis and survival under insulin deficiency and promotes β-cell regeneration. *eLife.* 3:3. https://doi.org/10.7554/eLife.03851

Zhang, F., D. Xu, L. Yuan, Y. Sun, and Z. Xu. 2014. Epigenetic regulation of Atrophin1 by lysine-specific demethylase 1 is required for cortical progenitor maintenance. *Nat. Commun.* 5:5815. https://doi.org/10.1038/ncomms6815

Zhang, H., E. Kang, Y. Wang, C. Yang, H. Yu, Q. Wang, Z. Chen, C. Zhang, K.M. Christian, H. Song, et al. 2016. Brain-specific Crmp2 deletion leads to neuronal development deficits and behavioural impairments in mice. *Nat. Commun.* 7.